Supporting Information

Aptamer conjugated polydopamine-coated gold nanoparticles as a dual-action nanoplatform targeting β-amyloid peptide for Alzheimer's disease therapy

Juan Qin [a, b], *Yanxue Guan* [a], *Zongjia Li* [a, b], *Xinyue Guo* [a, b], *Miaomiao Zhang* [a, *], *Dapeng Wang* [c, *], *Jilin Tang* [a, b, *]

[a] State Key Laboratory of Electroanalytical Chemistry, Changchun Institute of Applied Chemistry, Chinese Academy of Sciences, Changchun, 130022, P. R. China

[b] University of Science and Technology of China, Hefei, 230026, P. R. China

[c] State Key Laboratory of Polymer Physics and Chemistry, Changchun Institute of Applied Chemistry, Chinese Academy of Sciences, Changchun 130022, P. R. China

* Corresponding authors. E-mail addresses:

jltang@ciac.ac.cn (J. Tang)

mmzhang@ciac.ac.cn (M. Zhang)

wdp@ciac.ac.cn (D. Wang)

Materials

$A\beta_{1\text{-}40}$ powder was purchased from GL. Biochem Ltd. (Shanghai, China). 1,1,1,3,3,3-hexafluoro-2-propanal (HFIP) was purchased from Macklin Biochemical Co., Ltd. (Shanghai China). Thioflavin T (ThT) and Dulbecco's modified Eagle's medium (DMEM) cell culture medium was purchased from Sigma-Aldrich (St. Louis, MO). Chloroauric acid ($HAuCl_4 \cdot 3H_2O$) was purchased from Sinopharm Chemical Reagent Co., Ltd. (Beijing, China). Trisodium citrate, NaOH and NaCl were obtained from Beijing Chemical Reagent Factory (Beijing, China). Dopamine hydrochloride was purchased from Aladdin Reagent Co. (Shanghai, China). Tris (hydroxymethyl) aminomethane (Tris) was purchased from Beijing Dingguo Changsheng Biotech. Co., Ltd (Beijing, China). $A\beta_{1\text{-}40}$ aptamer (5'-SH-$(A)_6$-GGT GGC TGG AGG GGG CGC GAA CG-3') was synthesized by Sangon Biotech Co., Ltd (Shanghai, China). Fetal bovine serum (FBS) was from GIBCO BRL Life Technologies Inc. (Australia). Cell Counting Kit-8 (CCK-8) was purchased from Bioss (Beijing, China). 2',7'-dichlorofluorescein diacetate (DCFH-DA) were obtained from Beyotime Biotechnology (Nanjing, China). Aggregation buffer (pH=7.3) containing 10 mM Tris, 150 mM NaCl was freshly prepared at 25°C. All other chemicals and reagents were of analytical grade. Milli-Q-purified water (18.2 MΩ·cm) was used in all experiments.

Characterization of Au@PDA-Apt NPs

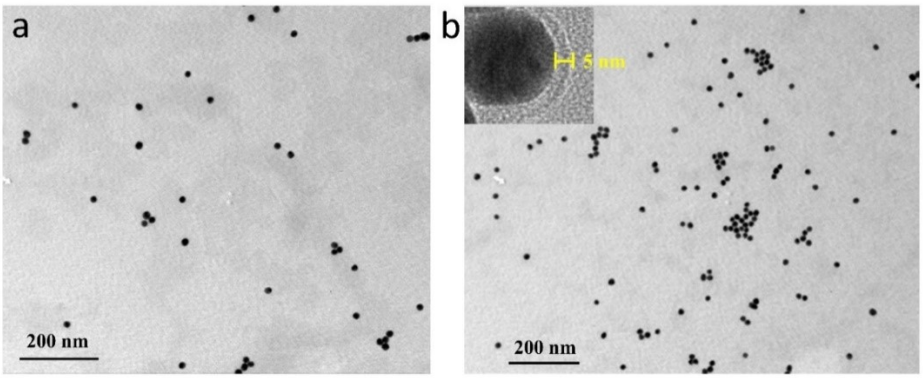

Fig. S1. (a) Low-magnification TEM images of AuNPs, (b) Low-magnification and high-magnification (inset) TEM images of Au@PDA-Apt NPs.

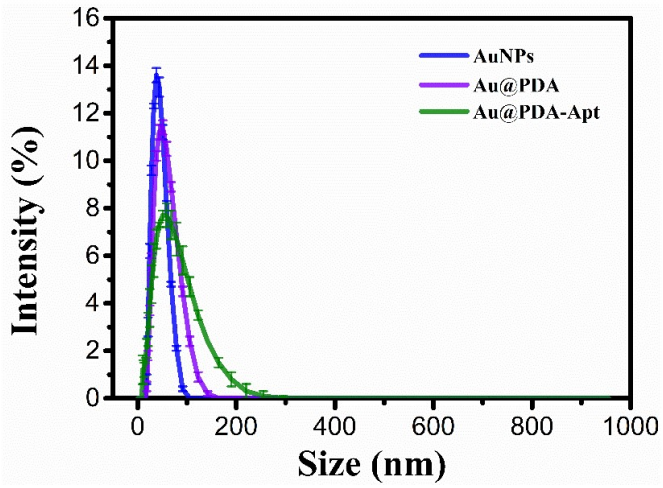

Fig. S2. The hydrodynamic size of AuNPs, Au@PDA and Au@PDA-Apt NPs.

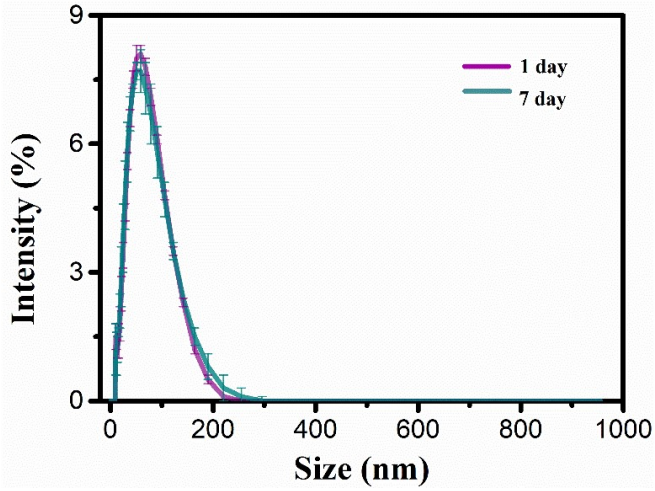

Fig. S3. The hydrodynamic size stability of Au@PDA-Apt NPs.

For the carbon peaks (C1 s), the increased intensity at ~286.2 eV (Au@PDA NPs or Au@PDA-Apt NPs v.s. bare AuNPs) was contributed by the C-O groups from PDA films on AuNPs surface (Fig. S1 a_1-a_3). In addition, the intensities of peaks at ~286.2 eV of Au@PDA-Apt NPs were both larger than those of Au@PDA NPs, indicating that aptamers were conjugated to Au@PDA NPs via the Michael addition reaction. Both Au@PDA NPs and Au@PDA-Apt NPs had nitrogen peaks (N1 s) at ~399.9 eV in the XPS spectra, but bare AuNPs did not, verifying the presence of PDA films (Fig. S1 b_1-b_3). Moreover, the nitrogen peaks of Au@PDA-Apt NPs were more intense than those of Au@PDA NPs, indicating aptamers successful conjugated on the surface of Au@PDA NPs.

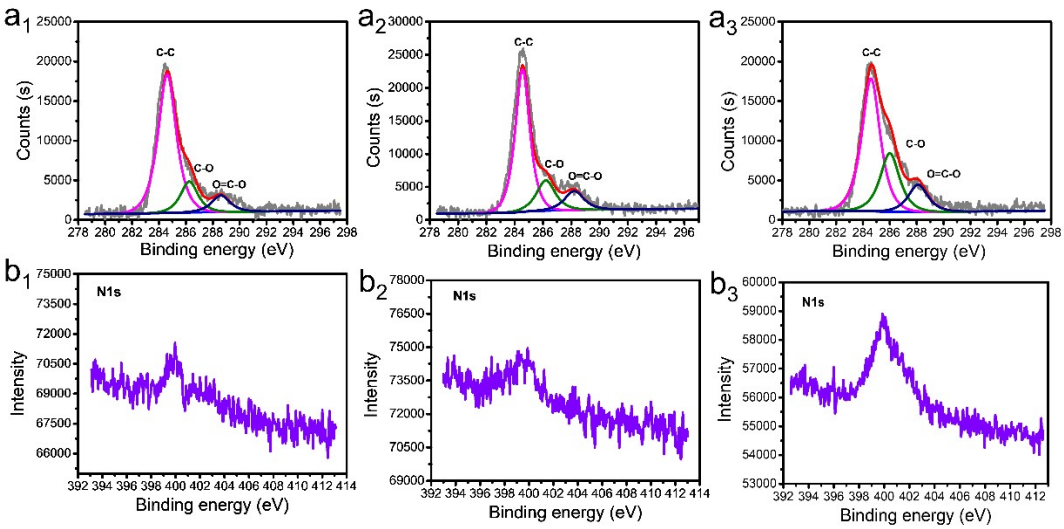

Fig. S4. XPS spectrum of nanoparticles. (a_1-a_3) narrow scan for C1s peaks of AuNPs, Au@PDA NPs and Au@PDA-Apt NPs, respectively. (b_1-b_3) narrow scan for N1s peaks of AuNPs, Au@PDA NPs and Au@PDA-Apt NPs, respectively.

ThT fluorescence

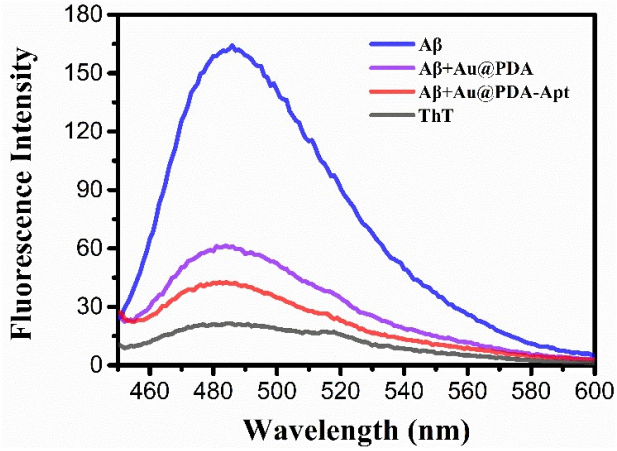

Fig. S5. ThT fluorescence intensity of $A\beta_{1-40}$ monomers incubated with 80 ug mL^{-1} Au@PDA NPs or Au@PDA-Apt NPs.

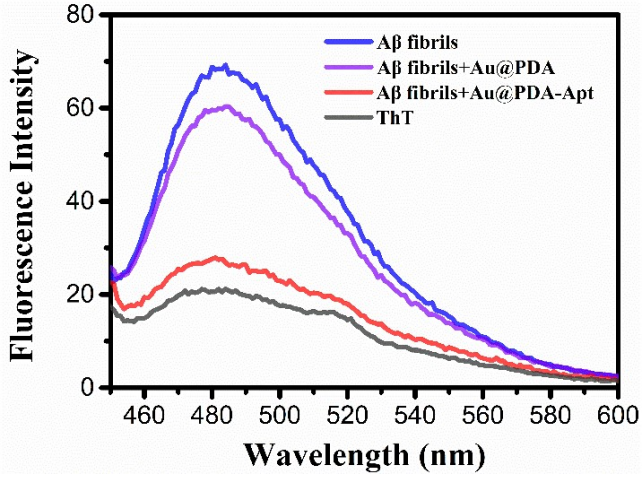

Fig. S6. ThT fluorescence intensity of $A\beta_{1-40}$ fibrils incubated with 80 μg mL^{-1} Au@PDA NPs or Au@PDA-Apt NPs for 12 h, respectively.

AFM imaging

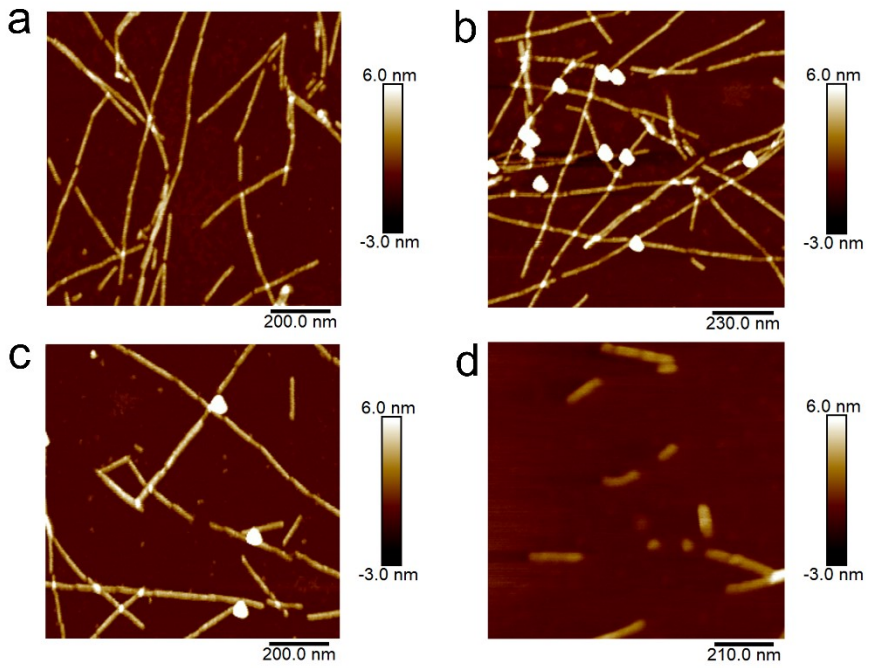

Fig. S7. AFM images of $A\beta_{1-40}$ incubated without (a), with 30 μg mL^{-1} (b), 50 μg mL^{-1} (c), and 80 μg mL^{-1} (d) of Au@PDA-Apt NPs for 7 days. Scale bar, 1 μm.

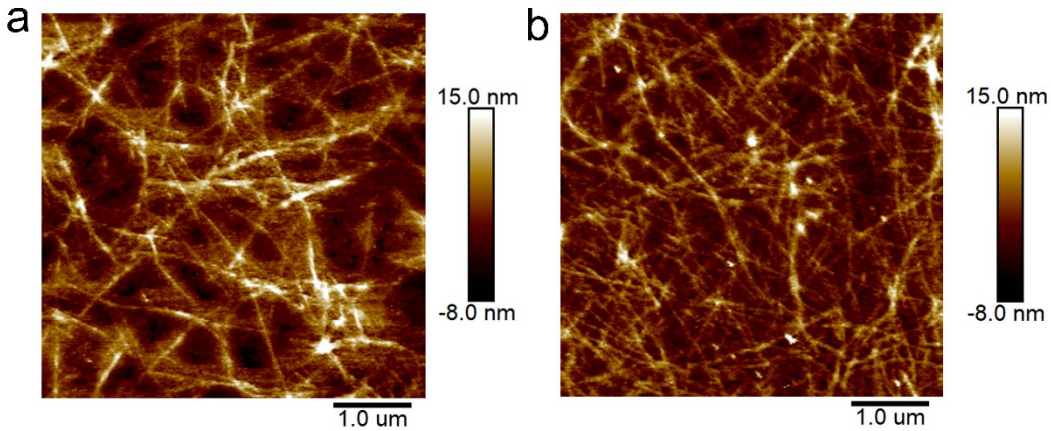

Fig. S8. AFM images of $A\beta_{1-40}$ monomers incubated without (a) and with (b) Aβ aptamer (0.1 μM) for 7 days.

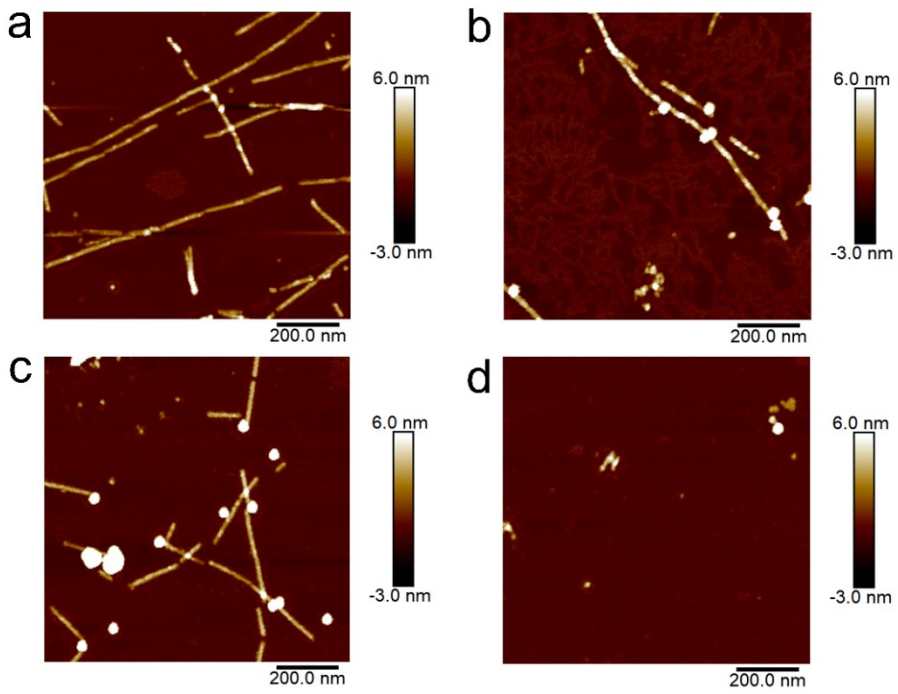

Fig. S9. AFM images of $A\beta_{1-40}$ fibrils incubated without (a), with 30 μg mL^{-1} (b), 50 μg mL^{-1} (c), and 80 μg mL^{-1} (d) of Au@PDA-Apt NPs for 12 h. Scale bar, 1 μm.

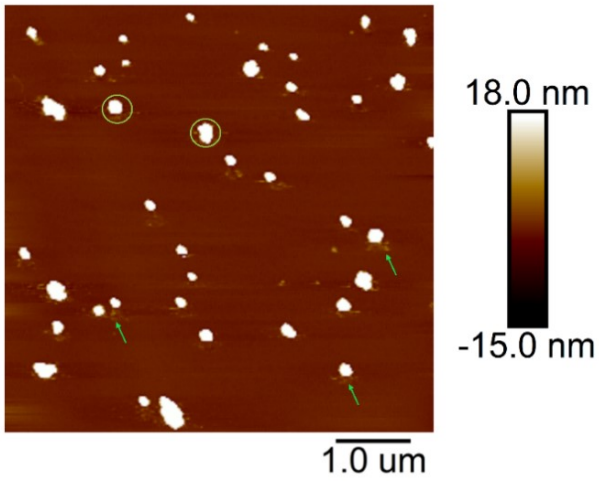

Fig. S10. AFM images of $A\beta_{1-40}$ fibrils incubated with 80 μg mL^{-1} Au@PDA-Apt NPs for 12 h.

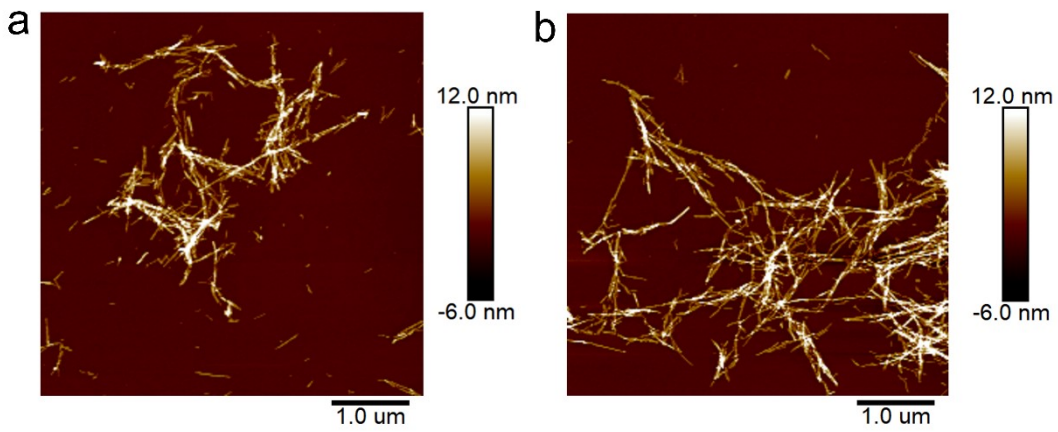

Fig. S11. AFM images of $A\beta_{1\text{-}40}$ fibrils incubated without (a) and with (b) Aβ aptamer (0.1 μM) for 12 h.

AFM Young's modulus data statistics

In each group of Young's modulus measurement, more than five cells were used to count. Each Young's modulus image was comprised of about 60,000 force-distance curves. Young's modulus for each pixel was obtained by fitting these force-distance curves. In this study, we used DMT model to fit force-distance curves and calculate Young's modulus of cells. The force fit boundary was 30%-90%.

The formula of DMT model to fit Young's modulus is as follow.

$$F_{\text{tip}} = \frac{4}{3} E \sqrt{R d^3} + F_{\text{adh}}$$

Where F_{tip} is the loading force, E is Young's modulus of the cell, F_{adh} is the adhesion force, R is the tip end radius and d is the tip-sample separation.

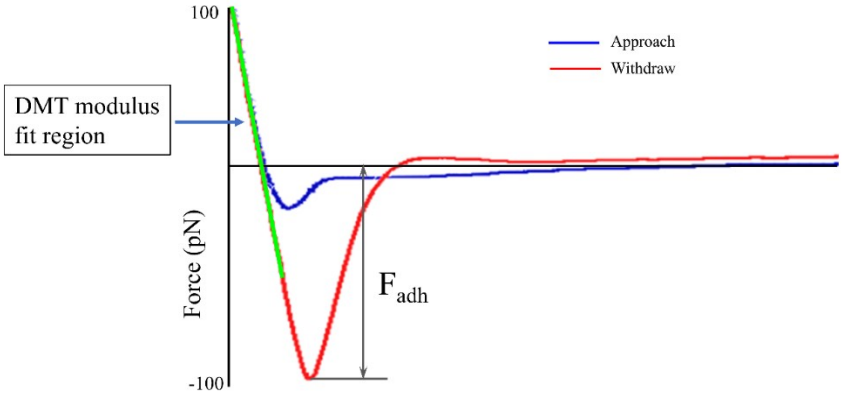

Fig. S12. Young's modulus fit from typical force-separation curve.

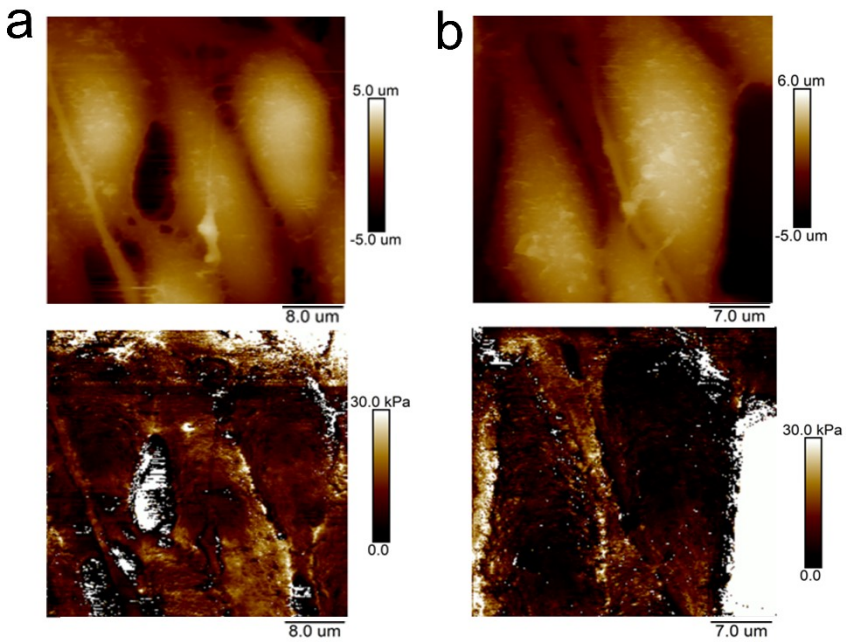

Fig. S13. The representative morphology images with corresponding Young's modulus mappings of PC12 cells treated with 80 μg mL^{-1} Au@PDA-Apt NPs.